GL00643

A MODEL FOR THE HEAT SOURCE OF THE CERRO PRIETO MAGMA-HYDROTHERMAL SYSTEM, BAJA CALIFORNIA, MEXICO

W. A. Elders*, D. K. Bird**, A. E. Williams* and P. Schiffman*
*Institute of Geophysics and Planetary Physics
University of California
Riverside, California 92521 U.S.A.
**Department of Geosciences
University of Arizona
Tucson, Arizona 85721 U.S.A.

Abstract

Earlier studies at Cerro Prieto by our group at UCR have led to the development of a qualitative model for fluid flow in the geothermal system before it was drilled and perturbed by production. Our current efforts are directed towards numerical modelling of heat and mass transfer in the system in this undisturbed state.

Our two-dimensional model assumes that the heat source was a single basalt/gabbro intrusion which provided heat to the system as it cooled. After compiling various information on the physical properties of the reservoir, we then calculated the enthalpy contained in two 1 cm thick sections across the reservoir orthogonal to each other. Next we considered various shapes, sizes and depths for the intrusion as initial conditions and boundary conditions for the calculations of heat transfer. A family of numerical models which so far gives the best matches to the conditions observed in the field today have in common a funnel-shaped intrusion with a top 4 km wide emplaced at a depth of 5 km some 30,000 to 50,000 years ago.

Our qualitative model postulated the existence of an inclined plume of hot geothermal water rising from the northeast with an inclination of 45°. This inclination, if due to the effect of regional groundwater, requires very high horizontal permeability. We believe, therefore, the component of horizontal flow is due largely to locally low permeability in the shallow surface rocks.

Our numerical modelling is still in progress. Although none of the models so far computed may be a perfect match for the thermal history of the reservoir, they all indicate that the intrusive heat source is young, close and large. Perhaps if nothing else, these models will stimulate the search for magma by geophysical means and possibly in the future by deep drilling.

Introduction

The Geothermal Resources group at the University of California, Riverside (UCR), has participated in the collaborative program of investigations of the Cerro Prieto geothermal field since 1977. During this time our emphasis has been upon petrological and geochemical study of borehole samples and surface emanations. We have applied the methods of hydrothermal mineralogy and petrology, fluid inclusion geothermometry, stable isotope geochemistry, vitrinite reflectance, fluid chemistry, fission track dating and interpretation of wireline logs toward the understanding of this hydrothermal system. Among the aims of our work were: (1) to assist in making lithological correlations between deep wells; (2) to improve the definition of the shape of the geothermal reservoir, as well as defining the nature of its boundaries; (3) to use a variety of geothermometric and dating methods to determine the thermal history of the field; (4) to determine various patterns of hydrothermal alteration which record the dynamics of fluid flow through the reservoir; and (5) to discuss the location and nature of the heat sources and how they couple with the geothermal system. These data are necessary input to modelling the natural circulation in the system as it was before exploitation. In turn such models are applicable to exploration, to assessment, to development, and to reservoir management.

Highlights of Our Earlier Work

Earlier findings from our studies at UCR were presented at the first three Symposia on Cerro Prieto in 1978, 1979 and 1981. However these publications dealt with only the first four of the topics listed in the previous paragraph. For example, at the First Symposium we reported on the regular sequence of mineral zones which form in response to increasing temperature within the field[1] and upon the use of oxygen and carbon isotopes to determine temperatures of equilibration between minerals and brines[2]. At the Second Symposium these ideas were expanded to use hydrothermal mineral zones to describe the shape and boundaries of the geothermal zone[3] and to use vitrinite reflectances to explore relative durations of heating across it[4]. Similarly a comprehensive study of the discharge of hot springs and other natural surface emanations from the reservoir was reported at that time[5].

At the Third Symposium the work of our group, in collaboration with other investigators, was extended to embrace a qualitative but comprehensive model of fluid flow for the Cerro Prieto field before production began[6,7,8,9,10,11,12]. This model was based upon (a) the location of the natural surface discharges in an arc west of the field[5,10]; (b) the temperature gradients measured in wells by the engineers of the Comision Federal de Electricidad (CFE)[13]; (c) the depths of the production zones in flowing wells reported by CFE[13]; (d) the depths to the first occurrence of various hydrothermal mineral zones, especially epidote and biotite[6]; (e) isotope and fluid inclusion geothermometry[7]; (f) the relative durations of heating from vitrinite reflectances[11]; (g) the

locations of zones of high and low electrical resistivity, based on downhole electrical logs[9]; (h) the location of intrusive dikes, in wells H2, NL-1, T-366 and M-189, along the eastern margin of the field[6]; (i) correlations with surface surveys of DC electrical resistivity by the geophysics group of Lawrence Berkeley Laboratory (LBL)[14]; and (j) the results of newer step out wells drilled by CFE.

Our Qualitative Flow Model

A key feature of this model is that we divided the field into four divisions: (i) an area of cold water recharge to the northeast; (ii) a zone of upward flowing boiling water in the center; (iii) a region of surface discharge lying to the west; and (iv) an aquifer in which flow of hot water is primarily horizontal, which lies at the extreme western boundary of the field (Figure 5 in Reference 6). We further inferred that this pattern was produced by hydrothermal convection in which a buoyant hydrothermal plume, dipping at 45° to the northeast, discharges to the southwest. Mass flow is recharged by cold water from the northeast which descends and is heated by a deep magmatic heat source in that direction (Figure 1).

Similarly our study of oxygen isotope data and of subsurface temperature data indicated that a reservoir volume of about 12 km^3 has exchanged its oxygen isotopes with water at temperatures greater than 200°C[7]. Based upon the measured isotope shifts between unreacted sediments and hydrothermally altered sediments, and upon the $\delta^{18}O$ of the waters, we calculated a water to rock mass ratio of 1.33 or a volume ratio of approximately 3. Thus 36 km^3 of water hotter than 200°C reacted with the 12 km^3 of the so far explored reservoir, causing the observed isotopic exchanges[7].

Our detailed studies of fission track annealing in detrital apatites in sandstones indicated that the well T-366 on the eastern side of the field went through the temperature range 160-180°C less than 10,000 years ago[8]. If this age can be generalized to the whole reservoir, it implies that the flux of >200°C water occurred in less than 10,000 years[8]. This in turn requires a flow of more than 36 billion liters of water a year through the whole reservoir in the natural state for approximately 10,000 years. If this fluid was flowing through a typical cross section of the reservoir averaging 6 km^2 in area, then the average flow rate would be 6 m/year. Because we believed that such a flow rate is similar to that which we expected for the subsurface flow of groundwater down the delta of the Colorado River from its apex near Yuma, Arizona, to Cerro Prieto, we further suggested that the inclination of the thermal plume, suggested in our model, was the resultant of the regional hydrologic gradient and the buoyancy forces of the geothermal system[6].

We have since quantified this inference as follows. In order to cause the resultant flow of the thermal plume to be inclined at 45°, the vertical momentum of the buoyant plume and the horizontal momentum of the cold river subflow must be equal. Yuma lies 57 km to the northeast and 33 m higher than the surface elevation of the Cerro Prieto field. If we assume ρ, the density of cold water, is 1.0 gm cm^{-3}, that μ, the coefficient of viscosity, is 0.0054 gm/cm (pure H_2O at 50°C and 200 bars), and that the delta has a uniform permeability, k, of 5×10^{-10} cm^2, we can calculate the velocity of the horizontal Darcy flow as

$$V = -k \left(\frac{\rho}{\mu}\right) g \frac{\Delta z}{\Delta x}$$
$$= 5.25\times10^{-8} \text{cm/sec} \approx 1.66 \text{ cm/year}.$$

Thus the average time for such water to traverse a 2 km horizontal distance would be about 12,000 years with this topographic gradient and permeability. If we assume the mean density of the hydrothermal water to be 0.7 gm cm^3 (ρ at 300°C with saturation pressure of 86 bars), for the horizontal velocity of the cold water given above, the vertical velocity of the thermal water must be 7.5×10^{-8}cm/sec (2.4 cm/year), an order of magnitude less than the velocity we estimated from our isotopic exchange and fission track annealing study. As we shall indicate later, it now seems unlikely to us that the indication of the thermal plume is caused solely by the interaction of the vertically flowing hot water and the horizontally flowing regional groundwater, as this requires the high horizontal permeability to persist at depth.

The Magma-Hydrothermal System

Our rough estimates of the heat stored in that part of this geothermal reservoir hotter than 200°C, down to a depth of 3 km, show that it is equivalent to the enthalpy contained in at least several of cubic kilometers of molten basalt. For such a large amount of heat to be transferred into the sediments in 10,000 years by convection also requires that the source of heat is both large and close. Therefore, the Cerro Prieto geothermal field should be considered as an active magma hydrothermal system.

Although the nearby Quaternary volcano of Cerro Prieto is a rhyodacite dome[15], we believe there are two compelling reasons for assuming that the heat source for the field is basaltic intrusions. Firstly, the dikes encountered in deep boreholes are largely diabases[6]. Secondly, in this tectonic setting of crustal spreading associated with "leaky" transform faults of the San Andreas fault - Gulf of California system, basalt intrusions are likely.

Ten years ago we postulated that this thermal anomaly lies in a "pull-apart basin" between the Cerro Prieto and Imperial faults[16]. If these faults move at rates comparable to the plate-edge deformations measured at the mouth of the Gulf of California, they have a spreading rate of about 5 cm/year implying a pull-apart rate of 10 cm/year for the "basin" or spreading center[16]. If the "basin" elongates in this way, it extends 1 km each 10,000 years. As the distance from the Cerro Prieto fault to the Imperial fault is about 15 km, this requires addition of a prism of new crust 1 km wide, 15 km long and up to 20 km deep (the approximate Moho depth) each 10,000 years. Suppose that this new crust is supplied from below by basalt magma from the mantle and from above by deltaic sediments of the Colorado River. A section of this prism only 3 km long and 1 km deep would

contain about the same amount of heat as 12 km^3 of the Cerro Prieto reservoir.

Modelling Heat and Mass Transfer

The prime criterion for successful calculations of the heat and mass transfer in the Cerro Prieto magma-hydrothermal system is that the observed conditions of temperature, pressure and the subsurface thermal energy in storage are replicated by our numerical analog models. Although the processes of heat and mass transfer in the earth's crust are irreversible processes and thus path dependent, constraints on the nature of the deep subsurface heat source and rock permeability can be made using simplifying approximations and making models which match the observed thermal regime in that part of the system so far explored by drilling. For computational simplicity we have restricted our calculations to two dimensions.

Our method is to critically evaluate: (1) the subsurface thermal energy in the Cerro Prieto field; and (2) thus to infer the possible nature of the magmatic heat source and the deep subsurface permeability that can replicate the observed distribution of temperature and pressure in the part of the system so far drilled.

Thermal Energy of the Cerro Prieto Geothermal System

Because we are interested in modelling the heat in storage before wells were drilled and production began, and because subjective decisions must commonly be made to infer equilibrium temperatures from downhole temperature logs, we have chosen to construct subsurface isotherms based on our isotopic data, using the calcite-water oxygen isotope geothermometer, and assuming fluid in the reservoir is isotopically well-mixed (Figure 2)[7]. Utilizing oxygen isotope temperatures for two approximately orthogonal cross-sections of the geothermal system presented in Figures 3 and 4 permits calculations of the thermal energy in the rock and fluid. The cross-sections are constructed for a SW to NE direction (CERRO1, Figure 3) and a SSE to NNW direction (CERRO2, Figure 4). Thus the first section (in Figure 3) is parallel to the horizontal component of the thermal plume and the second (in Figure 4) is perpendicular to the horizontal component of flow.

The total thermal energy of the Cerro Prieto geothermal field can be approximated by the following equation:

$$E_{th} = \int_0^V (\phi_T \rho_f H_f + [1-\phi_T]\, \rho_r H_r)\, dv$$

where ϕ_T = total porosity
ρ_f = fluid density, gm/cm^3
H_f = fluid enthalpy, cal/cm
ρ_r = rock density, gm/cm^3
H_r = rock enthalpy, cal/cm

Our thermal energy calculations for Cerro Prieto are normalized to 1 cm^3 of rock and fluid-filled pores where

$$\text{Fluid energy} = \phi_r \rho_{H_2O} \left(H_{H_2O,T,P} - H^0_{H_2O,T^0,P^0}\right)$$

$$\text{Rock energy} = (1-\phi_T)\rho_r\, C_{p_r}\, (T-T_0)$$

Total energy = Fluid energy + Rock energy

$$H_{r,T,P} - H^0_{r,T^0,P^0} = \int_{T^0,P^0}^{T,P} C_{p_r}\, dT,$$

assuming Cp_r is constant with a time and volume averaged $\overline{Cp}^0$. The calculated energy values approximate the total anomalous thermal energy referenced to a background geothermal gradient of 25°C/km for each grid point.

The two orthogonal cross-sections (Figures 3 and 4) through the Cerro Prieto geothermal field utilize a 15 x 20 grid covering a lateral distance of ∿7 km and a vertical depth of 2 km. The temperatures from the oxygen isotope and other geochemical data[6,7] were input to a program which retrieves fluid properties. Thermodynamic data for H_2O are calculated using saturation pressures for the temperature values[17,18].

Values for porosity have been approximated from drillhole and geophysical data[19]. Similarly we chose values of the heat capacity for rock as a function of temperature and rock composition, using published heat capacity data[20].

Rock Density and Porosity

An average grain density value was computed using a typical sand composition from Cerro Prieto drillhole cuttings, and mineral density values from reference 21. Both altered and unaltered grain densities averaged 2.7 gm/cm^3 which shows the dominance of quartz and feldspar in the sand composition.

Measured values for porosity of cores as a function of depth were reported for several drillholes at Cerro Prieto[19]. These values range from 5% to 40% between surface and 2 km depth. Using the porosity-depth trends in wells M-96 and M-127 reported in reference 19, a grid of porosity values was determined for the cross-sections in Figures 3 and 4.

Heat Capacity

Heat capacity of rocks varies with mineralogy and temperature. For the Cerro Prieto geothermal field an average composition of Colorado River delta sand was used to compute heat capacity of the sands at different temperatures. Heat capacities were computed for both altered and unaltered samples. For a 300°C sample, variations of heat capacity range from .238 to .284 cal/cm°C. Unaltered samples at less than 300°C ranged from .204 to .24. We used an average value of .25 cal/gm°C as an acceptable approximation, based on these calculations.

It is evident in Figures 3 and 4 that the topology of the thermal energy sections is strongly controlled by the isotherms. The maximum energy in the fluid phase is about 55 cal/cm^{-3}, which represents about a third of the total thermal energy in the system at porosities of 30%. The effect of decreasing fluid density opposes the effect of increasing standard molal heat capacity

of water with increasing temperatures at low pressures. Thus the thermal energy of the fluid decreases with increasing temperature at 345°C.

Geologic Characteristics Used in the Numerical Analog Models

Our preliminary calculations of heat and mass transfer presented below were designed to approximate a geologic cross-section 16 km long and 10 km deep along an approximate NW-SE section through the geothermal field, east of the Cerro Prieto fault. This numerical section was chosen to be parallel to the regional tensional stresses and perpendicular to the numerous dip slip faults within and near the production zone. Because this section is nearly perpendicular to the assumed regional groundwater flow in the delta, complications of this hydrologic gradient are minimized for these preliminary calculations. As is seen in Figure 4, the pattern of isotherms in this cross-section is approximately bilaterally symmetrical.

The observed and inferred stratigraphy, structure and temperature distributions for this cross-section are summarized in Figure 5. Note that the high angle normal faults are centered about the shallow subsurface thermal anomaly, and that these faults apparently offset the postulated three major geologic units. These are Unit A (unconsolidated sediments), Unit B (consolidated sediments), and granite basement, as defined by De la Peña *et al.*[22] and Lyons and Van de Kamp[19]. The location of the basement is based upon the work of Fonseca and Razo[23] and the seismic basement is after that shown by Prian[24]. The 300°C isotherm is locally within 2 km from the surface. It can be inferred from Figure 5 that at 2.5 km depth this isotherm extends over a cross-sectional distance of about 4 km or more.

Preliminary Numerical Analysis

For ease of calculation we have limited the calculations to two dimensions and assumed that the heat source was emplaced as a single event.

In order to rapidly and inexpensively evaluate the nature of possible magmatic heat sources and the subsurface permeability distribution, the numerical section was divided into only forty internal grid points. Each point represents the volume averaged thermodynamic and transport properties of a representative elementary volume of rock and fluid 0.001 km thick and either 2 x 2 km or 1 x 1 km in area. Calculations are made using the computer program FLOW51 and the graphics support developed by Norton and Knight at the University of Arizona[25]. All boundary conditions were chosen to be conductive to heat transfer with various combinations of open or closed boundaries to fluid flow. The surface temperature is 20°C and the initial regional temperature gradient is 25°C per kilometer.

Nature of the Heat Source

The calculations presented below evaluate the effects of various permeability distributions in the upper 10 km of the earth's crust on the dispersion of thermal energy from a tholeiitic basaltic magma intrusion whose dimensions are arbitrarily chosen. The initial temperature of the intrusion is 1150°C which crystallizes during a temperature drop of about 100 to 150°C to release about 100 cal/gm due to the heat of crystallization[21,26]. For a time and volume averaged heat capacity of a gabbro of 0.25 cal/gm°C the intrusion will release about 330 cal/gm to cool to an average ambient temperature of ~220°C. We can then vary the dimensions and locations of the intrusion and observe the propagation of heat into the Cerro Prieto reservoir at successive time steps.

Initially we calculated the cooling history of vertical diabase dikes intruding the sediments at various levels. This analysis showed that however the dikes cooled, by conduction, or by both conduction and convection, such dikes rapidly lose most of their heat by horizontal conduction. Even a dike 1 km thick would contain too little enthalpy and would cool too fast to be the heat source for the Cerro Prieto reservoir. This led us to consider larger basalt intrusions in close proximity. To give rise to the heat contained in the cross-section across Cerro Prieto, we need an intrusion which is at least 4 km by 4 km in cross-section and emplaced no deeper than 6 km. This assumption is consistent with the heat required to provide the heat in storage in the drilled section of the geothermal field. The total energy of the 4 km by 4 km by 1 cm thick cross-section of the pluton is about 4×10^{13} calories (Figure 6A).

The maximum temperatures in the numerical cross-section that result from the conductive cooling of this type of intrusion (thermal conductivity = 6×10^{-3} cal/°C) are shown in Figure 6B. Note that the 300°C isotherm progresses <2 km above the intrusion which is >4 km from the surface. The effects of convection on the thermal energy transfer from this intrusion are given below.

Maximum Temperatures with Convection

The effects of permeability with an open top boundary (i.e., no caprock) on the maximum temperature distributions for four different models are shown in Figures 7A and 7B for each model. The permeability structure representative of 2 km by 2 km representative elementary volumes (REV's) over the 16 km by 10 km numerical cross-section are given. The distribution of permeability reflects the general structural characteristics given in Figure 5. The volume averaged permeability of the 2 km by 2 km REV's are: Unit A, $k = 10^{-10}cm^2$; Unit B, $k = 10^{-11}cm^2$; and the granitic basement, $k = 10^{-12}cm^2$. High angle normal faults associated with the subsurface thermal energy anomaly are represented by higher permeabilities shown in Figures 7A and 7B. Permeabilities of the intrusion of 10^{-13} to $10^{-12}cm^2$ begin to be realized at a fracture temperature of 1000°C in the crystallized basalt or gabbro (after Norton and Taylor, 1978)[26]. Note that the intrusions in numerical models CPP1 and CPP2 have permeabilities of $10^{-13}cm^2$, but in models CPP3 and CPP4 the top half of the intrusion

has a permeability of $10^{-12}cm^2$.

The permeabilities of the host rocks lateral to the intrusion are equivalent for all models with the exception of CPP3, where higher permeabilities are assigned to the host rocks near the base of the cross-section. Similarly, the permeability structure above the intrusion is the same for all the sections illustrated in Figure 7 with the exception of CPP2 where higher permeabilities were chosen.

The maximum temperatures throughout the numerical domain as a result of cooling the same intrusion with the four different permeability structures are also illustrated in Figure 7. Note that none of the models replicate exactly the observed subsurface temperatures observed in the Cerro Prieto geothermal system. Nevertheless these calculations do give somewhat similar results to the actual subsurface conditions of the present thermal energy anomaly at Cerro Prieto.

Effects of permeability variations directly above the intrusion can be seen in comparing models CPP1 and CPP2. Because the permeability within and lateral to the intrusion are equivalent in these models, the flux of thermal energy through the top of the intrusions is approximately the same for both CPP1 and CPP2. As a consequence of the higher permeabilities of CPP2 the thermal energy flux through the top of the intrusion is rapidly dispersed. Note that the 300°C isotherm in CPP2 progresses only ∿1.5 km above the intrusion, which is less than that observed for the conductive cooling (Figure 6). In CPP1, which has lower permeabilities, the 300°C isotherm advances about 2.2 km above the intrusion. It is apparent from these calculations that the permeabilities within and lateral to the intrusion need to be known if this $4x10^{13}$ calorie energy source is to replicate the observed temperature distribution at Cerro Prieto.

The consequences of increasing the permeability within and lateral to the intrusion are shown in Figure 7 by comparing the results of CPP3 and CPP4 with CPP1. In all three of these models the permeability structure above the intrusion is the same. Note in CPP3 that the 300°C isotherm advances ∿3.3 km above the intrusion to within about 2.7 km of the surface. This 300°C isotherm is <3 km wide at its highest point and thus the model does not provide the necessary thermal energy transfer to the shallow subsurface as required by observations from drillholes at Cerro Prieto. It is apparent in these numerical approximations that the permeabilities within and lateral to the intrusive heat source are critical to the style of thermal energy transport in these magma-hydrothermal systems.

Calculated temperatures at depths of 1, 2, and 3 km from the surface directly above the intrusive heat source are given in Figure 8 as a function of time after the intrusion. In all four models the intrusion cools below 1000°C and fractures to give the assigned permeability at ∿70,000 ± 5,000 years. Maximum rates of change of temperatures in the upper 3 km of the earth's crust above these intrusions occurs just after the fracturing of the intrusion. Maximum temperatures in the shallow subsurface occur within 10,000 to 20,000 years after the intrusion cools to <1000°C (Figure 8). Note that temperatures >275°C at 3 km depth in CPP1, CPP3, and CPP4 occur for times of <10,000 years after fracturing of the pluton.

It is apparent from these preliminary calculations that the observed thermal anomaly at Cerro Prieto cannot be explained exactly by a cross-sectional energy source of $4x10^{13}$ calories at 6 to 10 km deep, with reasonable permeability structures in the upper 10 km of the earth's crust with the boundary conditions shown in Figure 4. Increasing the permeability of the intrusion and the adjacent host rocks will increase the thermal energy transfer to the shallow subsurface, but values larger than that shown in CPP3 (Figure 7) are not justifiable[26]. Consequently, for the boundary conditions chosen the ultimate energy source for the Cerro Prieto geothermal system must be $>4x10^{13}$ calories. We have therefore considered a larger heat source in the numerical model presented below, and also considered the effects of the depth of the heat source and of a closed top boundary.

Revised Numerical Models

In view of the results presented above, an expanded numerical cross-section was employed to evaluate the consequences of depth to a larger heat source. These models have 80 internal grid points, each denoting a representative elemental volume of 1 km by 1 km x 0.001 km. Three different heat sources emplaced at different depths from the surface are considered. The permeability structures chosen are given in Figures 9, 10 and 11. Note that it has been modified relative to the CPP1 to CPP4 models. Unit A has a permeability of $10^{-11}cm^2$ and for Unit B $k = 5x10^{-12}cm^2$. Also a higher permeability for the geothermal reservoir of 10^{-10} was chosen. Other than these differences the general permeability structure is similar to the earlier models. An important difference in these models is in the top boundary condition which is chosen as a no-flow boundary (see Figures 9, 10 and 11).

It is apparent from the calculated isotherms given in Figures 9, 10 and 11 that the closed top boundary condition results in a very wide dispersal of heat in the upper 2 to 3 km of the numerical sections. The temperature gradient reversals in the upper 3 km are a consequence of the lateral migration of fluids due to the impermeable top boundary and mass recharge by cold groundwater at depths of 2.5 to 3 km. Because heat can only be transferred by conduction through the top boundary, high temperatures occur in the shallow subsurface over a very large portion of the cross-section. For example, the 200°C isotherm extends for >10 km in width at <1 km deep in the three models shown in Figures 9, 10 and 11 at 100,000 years after the intrusion. The width of the 300°C isotherm is also instructive. Its maximum width in the upper 3 km is >4.5 km as opposed to the 3 km actually observed at Cerro Prieto. It would appear therefore that the heat source must be smaller or deeper than that represented in models CPP5, CPP6 and CPP7.

Whereas Figures 9, 10 and 11 (models CPP5, CPP6 and CPP7) depict three different sizes of the heat source for impermeable surface boundary conditions, models CP41, CP42 and CP43 depict more realistic shapes for a gabbro/basalt intrusion which commonly are funnel-shaped[26,27,28,29]. The plutons in Figures 12, 13 and 14 are smaller than those in the Figures 9, 10 and 11. The boundary condition also differs in that the surface is open to fluid flow. The numerical cross-section of CP42 has a low permeability surface zone of 0.1 md above the intrusion. As can be seen from these Figures, these boundary conditions give a closer approximation between temperatures calculated for the model and the observed temperatures in the downhole logs. In all three cases the width of the thermal plume is approximately correct after 30,000 years have elapsed. The low permeability zone above the intrusion in model CP41, which acts as a leaky caprock, gives a thermal plume of approximately the correct width and rise time. However, the model CP43 (Figure 14) which has an impermeable caprock, seems to give an even better fit.

We are currently evaluating the transport and thermodynamic characteristics of various other models in order to improve our predictive estimates of the nature and location of the heat source and how it relates to the Cerro Prieto magma-hydrothermal system. Models with a 500 m grid spacing will help give a higher degree of resolution. Similarly models including horizontal regional groundwater flow are in progress.

Conclusions

The very high temperatures at shallow depth in the Cerro Prieto geothermal field suggest that there should be a heat source which is a young, large, nearby igneous intrusion. Our preferred model at present is that it is a funnel-shaped gabbro intrusion, probably 30,000 to 50,000 years old, some 4 km across at a depth of 5 km. Above it there is probably a sheeted dike complex as is typical of ophiolite complexes in ocean spreading centers[28,29]. Our numerical models for simplicity assumed that there was a single intrusive event which is now cooling. If, as is likely in a tectonic setting of crustal spreading, there have been repeated incursions of magma for a long period, then the intrusion must be even larger and older. Whatever its form, the existence of the igneous intrusion seems to us to be inevitable. It should be detectable geophysically and perhaps in the future may be found to be accessible by deep drilling. Perhaps before the next century it will be found to be a viable energy source.

Acknowledgments

Our work at Cerro Prieto is currently funded by Department of Energy contract nos. DE-FC07-80ID12145 and DE-AT03-80SF11458. We thank our numerous colleagues in CFE, LBL and elsewhere, with whom we have had the privilege of being associated in the cooperative study of Cerro Prieto. This is report no. 82/9 of the Institute of Geophysics and Planetary Physics of UCR.

References

(1) W. A. Elders, J. R. Hoagland, S. D. McDowell and J. M. Cobo, Hydrothermal mineral zones in the geothermal reservoir of Cerro Prieto, B.C., Mexico. 1979 Geothermics, v. 8, p. 201-209.

(2) E. R. Olson, Oxygen and carbon isotope studies of calcite from the Cerro Prieto geothermal field, Baja California, Mexico. 1979 Geothermics, v. 8, 7 p.

(3) W. A. Elders, J. R. Hoagland and A. E. Williams, The distribution of hydrothermal mineral zones in the Cerro Prieto geothermal field of Baja California, Mexico. 1981 Geothermics, v. 10, no. 3/4, p. 245-254.

(4) C. E. Barker and W. A. Elders, Vitrinite reflectance geothermometry and apparent heating duration in the Cerro Prieto geothermal field. 1981 Geothermics, v. 10, no. 3/4, p. 207-224.

(5) J. N. Valette and I. Esquer-Patiño, Geochemistry of the surface emissions in the Cerro Prieto geothermal field. Proceedings of the Second Symposium on the Cerro Prieto Geothermal Field, Oct. 1979, Mexicali, p. 241-254.

(6) W. A. Elders, A. E. Williams and J. R. Hoagland, An integrated model for the natural flow regime in the Cerro Prieto geothermal field, B.C., Mexico, based upon petrological and isotope geochemical criteria. UCR/IGPP report 81/8. In press, Proceedings of the Third Symposium on Cerro Prieto, March 1981, San Francisco.

(7) A. E. Williams and W. A. Elders, Oxygen isotope exchange in minerals from the Cerro Prieto geothermal system: Indicator of temperature distribution and fluid flow. UCR/IGPP report 81/9. In press, Proceedings of the Third Symposium on Cerro Prieto, March 1981, San Francisco.

(8) S. J. Sanford and W. A. Elders, Dating thermal events by fission track annealing in wells M-94 and T-366 at Cerro Prieto. UCR/IGPP report 81/10. In press, Proceedings of the Third Symposium on Cerro Prieto, March 1981, San Francisco.

(9) D. T. Seamount, Jr. and W. A. Elders, Well log use at Cerro Prieto in identification of hydrothermally altered zones, correlation with reservoir temperature and interpretation of reservoir porosity. UCR/IGPP report 81/11. In press, Proceedings of the Third Symposium on Cerro Prieto, March 1981, San Francisco.

(10) J. N. Valette-Silver, I. Esquer-Patiño, W. A. Elders, P. C. Collier and J. R. Hoagland, Hydrothermal alteration of sediments associated with surface emissions from the Cerro Prieto geothermal field, Baja California, Mexico. UCR/IGPP report 81/12. In press, Proceedings of the Third Symposium on Cerro Prieto, March 1981, San Francisco.

(11) C. E. Barker, M. J. Pawlewicz, N. H. Bostick and W. A. Elders, Evolution of the Cerro Prieto Geothermal System as interpreted from vitrinite reflectance under isothermal conditions. In press, Proceedings of the Third Symposium on Cerro Prieto, March 1981, San Francisco.

(12) J. N. Valette-Silver, J. N. Thompson and J. W. Ball, Relationship between water chemistry and mineralogyin the superficial part of the Cerro Prieto geothermal field. In press, Proceedings of the Third Symposium on Cerro Prieto, March 1981, San Francisco.

(13) F. J. Bermejo M., F. X. Navarro O., F. Castillo B., C. A. Esquer y C. Cortez A., Variacion de Presion en el yacimento de Cerro Prieto durante su explotarion. Actas del Segundo Simposia sobre el Campo Geotermico de Cerro Prieto, Baja California, Mexico, Oct. 1979, Mexicali, p. 473-496.

(14) M. J. Wilt and N. E. Goldstein, Resistivity modelling at Cerro Prieto. Proceedings of the Second Symposium on Cerro Prieto, Oct. 1979, Mexicali, p. 419-436.

(15) W. A. Elders, J. R. Hoagland, E. R. Olson, S. D. McDowell and P. Collier, A comprehensive study of twenty-three wells in the Cerro Prieto Geothermal Field, Baja California, Mexico. UCR/IGPP report 78/26, 1978.

(16) W. A. Elders, R. W. Rex, T. Meidav, P. T. Robinson and S. Biehler, Crustal spreading in southern California. The Imperial Valley and Gulf of California formed by rifting apart of a continental plate. Science, v. 178, no. 4056, p. 15-24, 1972.

(17) J. H. Keenan, F. G. Keyes, P. F. Hill and J. G. Moore, Steam Tables: Thermodynamic Properties of Water Including Vapor, Liquid and Solid Phases. John Wiley & Sons, 1969.

(18) H. C. Helgeson and D. H. Kirkham, Theoretical prediction of the thermodynamic behaviour of aqueous electrolytes at high pressures and temperatures. Am. J. Sci., v. 274, p. 1089-1198, 1979.

(19) D. J. Lyons and P. C. Van de Kamp, Subsurface geological and geophysical study of the Cerro Prieto geothermal field, Baja California, Mexico. Lawrence Berkeley Laboratory report no. 10540, 1980.

(20) H. C. Helgeson, J. M. Delany, H. W. Nesbitt and D. K. Bird, Summary and critique of the thermodynamic properties of rock-forming minerals. Am. J. Sci., v. 278-A, 1978.

(21) S. P. Clark, Handbook of physical constants, Revised Edition, Geol. Soc. Amer. Memoir 97, 1966.

(22) A. de la Peña L., I. Puente C., y E. Diaz C., Modelo del campo geotermico de Cerro Prieto. Proceedings of the Second Symposium on the Cerro Prieto Geothermal Field, Oct. 1979, Mexicali, p. 29-56.

(23) H. L. Fonseca L. y A. Razo M., Estudios gravimetricos, magnetometricos y de sismica de reflexion en el Campo Geotermico de Cerro Prieto. Proceedings of the Second Symposium on the Cerro Prieto Geothermal Field, Oct. 1979, Mexicali, p. 303-328.

(24) R. Prian C., Posibilidades de desarrollo del area geotermico de Cerro Prieto, Baja California Norte. Proceedings of the Second Symposium on the Cerro Prieto Geothermal Field, Oct. 1979, Mexicali, p. 146-161.

(25) D. Norton and J. Knight, Transport phenomena in hydrothermal systems: Cooling plutons. Am. J. Sci., v. 277, 1977.

(26) D. Norton and H. P. Taylor, Quantitative simulation of the hydrothermal systems of crystallizing magmas on the basis of transport theory and oxygen isotope data: An analysis of the Skaergaard intrusion. J. Petrol., v. 20, no. 3, p. 421, 1979.

(27) L. R. Wager and G. M. Brown, Layered Igneous Rocks. W. H. Freeman and Co., 1968.

(28) J. S. Pallister and C. A. Hopson, Samail ophiolite plutonic suite field relations, phase variation, cryptic variation and layering, and a model of a spreading ridge magma chamber. J. Geophys. Res., v. 86, p. 2594, 1981.

(29) R. G. Coleman, Tectonic setting for ophiolite subduction in Oman. J. Geophys. Res., v. 86, p. 2497, 1981.

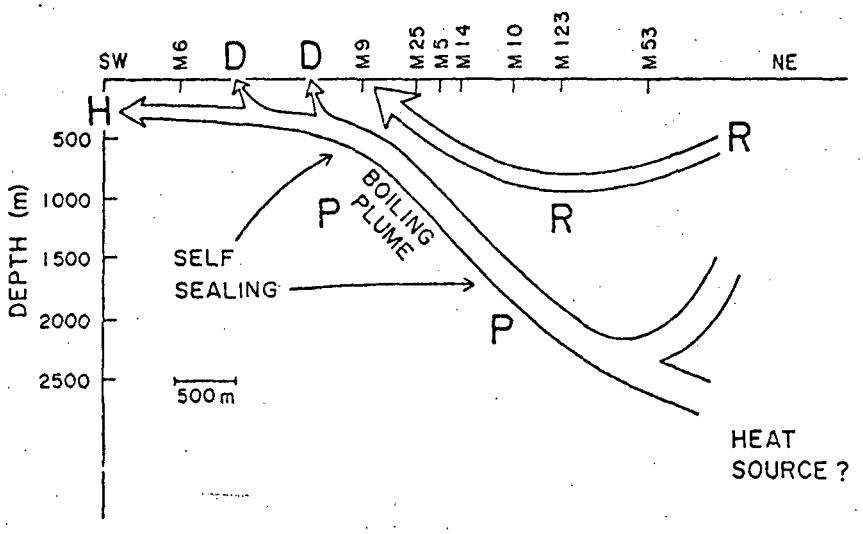

Figure 1. SW-NE cross-section showing the flow regime proposed for Cerro Prieto (from Reference 6).

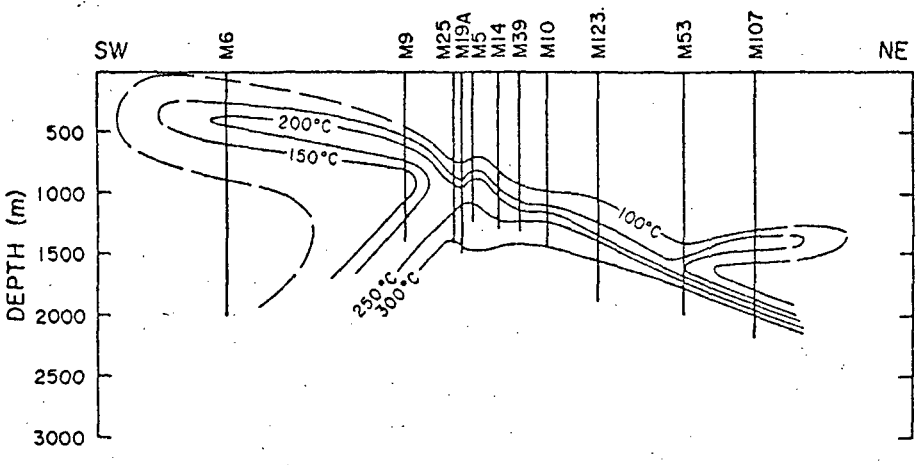

Figure 2. Isotherms on the same profile as Figure 1. Based on the calcite-water isotopic geothermometer (after Reference 7).

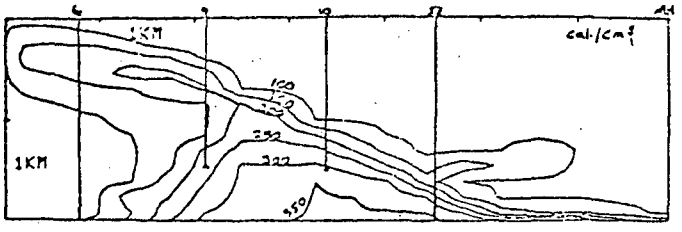

TEMPERATURE CENTIGRADE

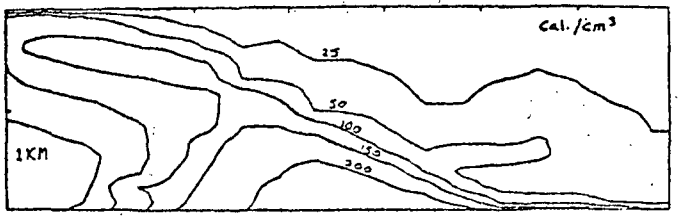

TOTAL ENERGY

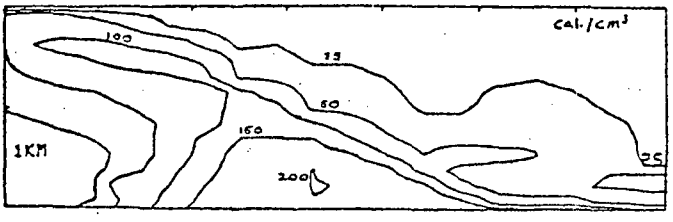

ROCK ENERGY

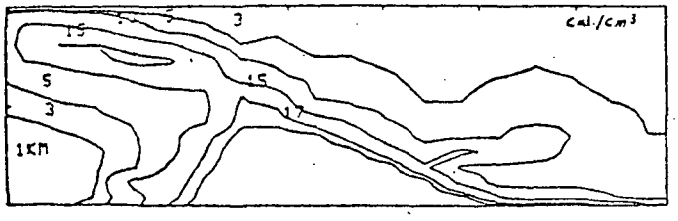

FLUID ENERGY

Figure 3. Temperature and energy sections across the field from SW to NE.

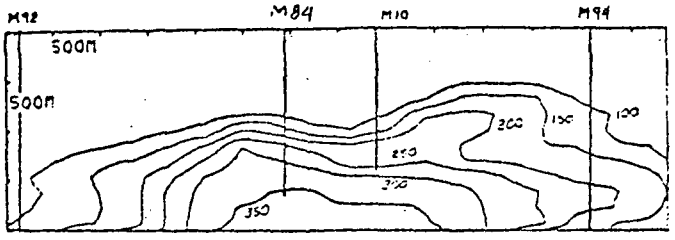

TEMPERATURE CENTIGRADE

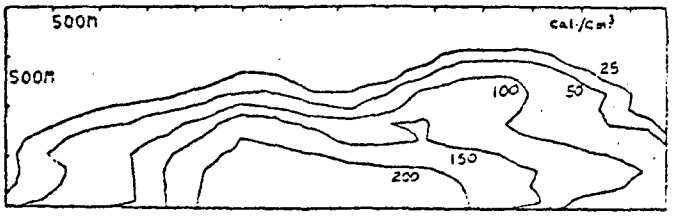

TOTAL ENERGY

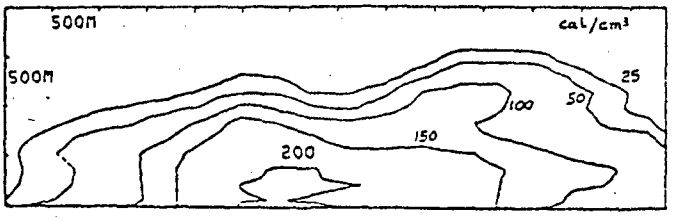

ROCK ENERGY

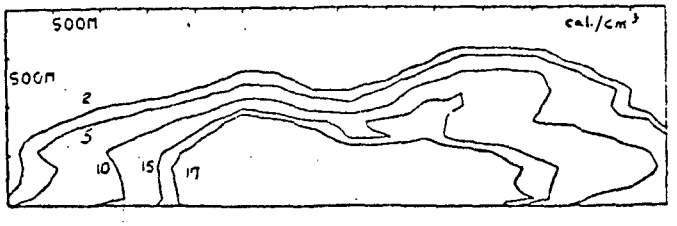

FLUID ENERGY

Figure 4. Temperature and energy sections across the field from NW to SE.

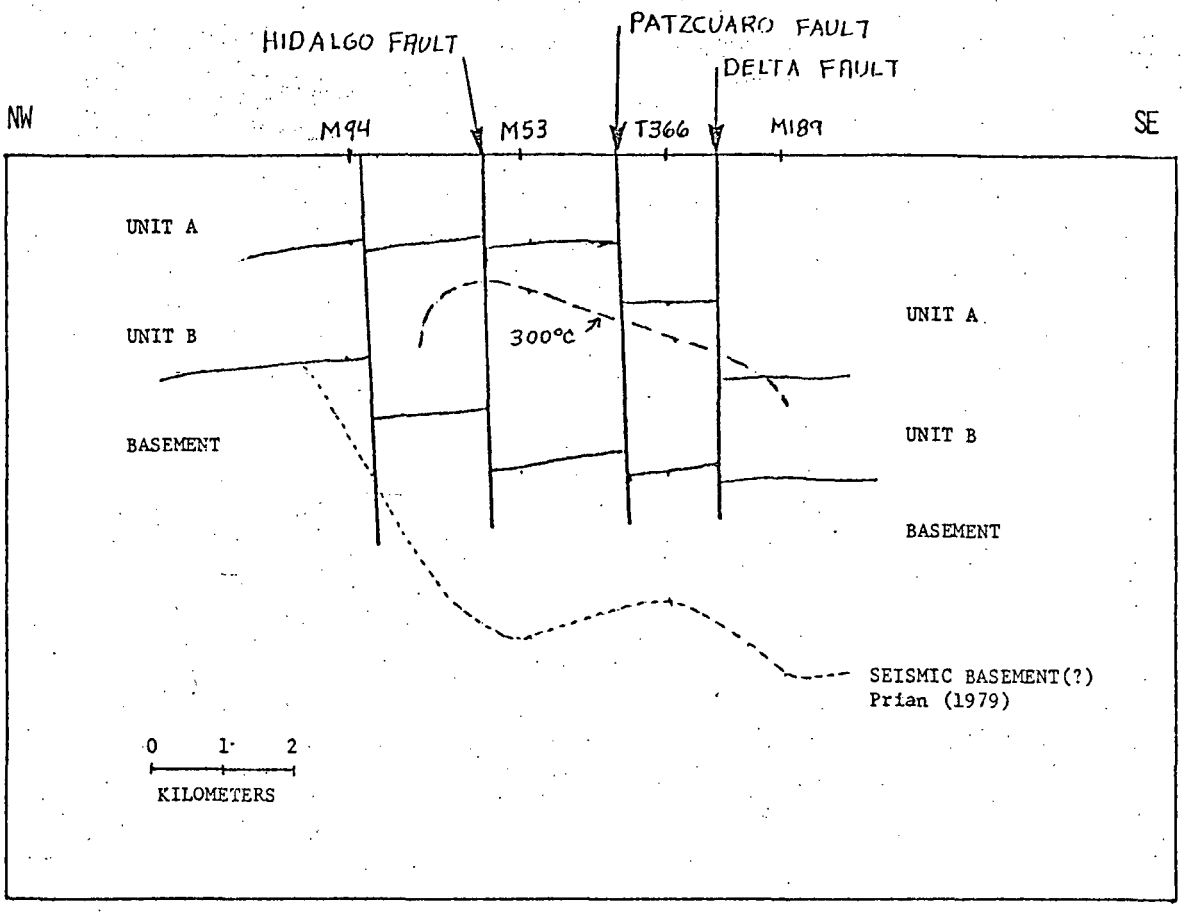

Figure 5. Schematic geologic cross-section from NW to SE across the field (after References 19, 22, 23 and 24).

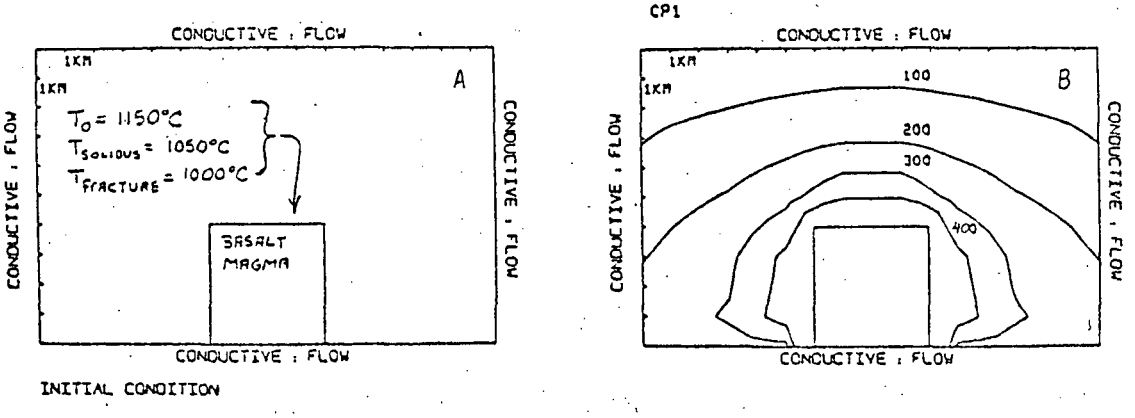

Figure 6. Initial conditions (A) and maximum temperatures (B) for conductive cooling model.

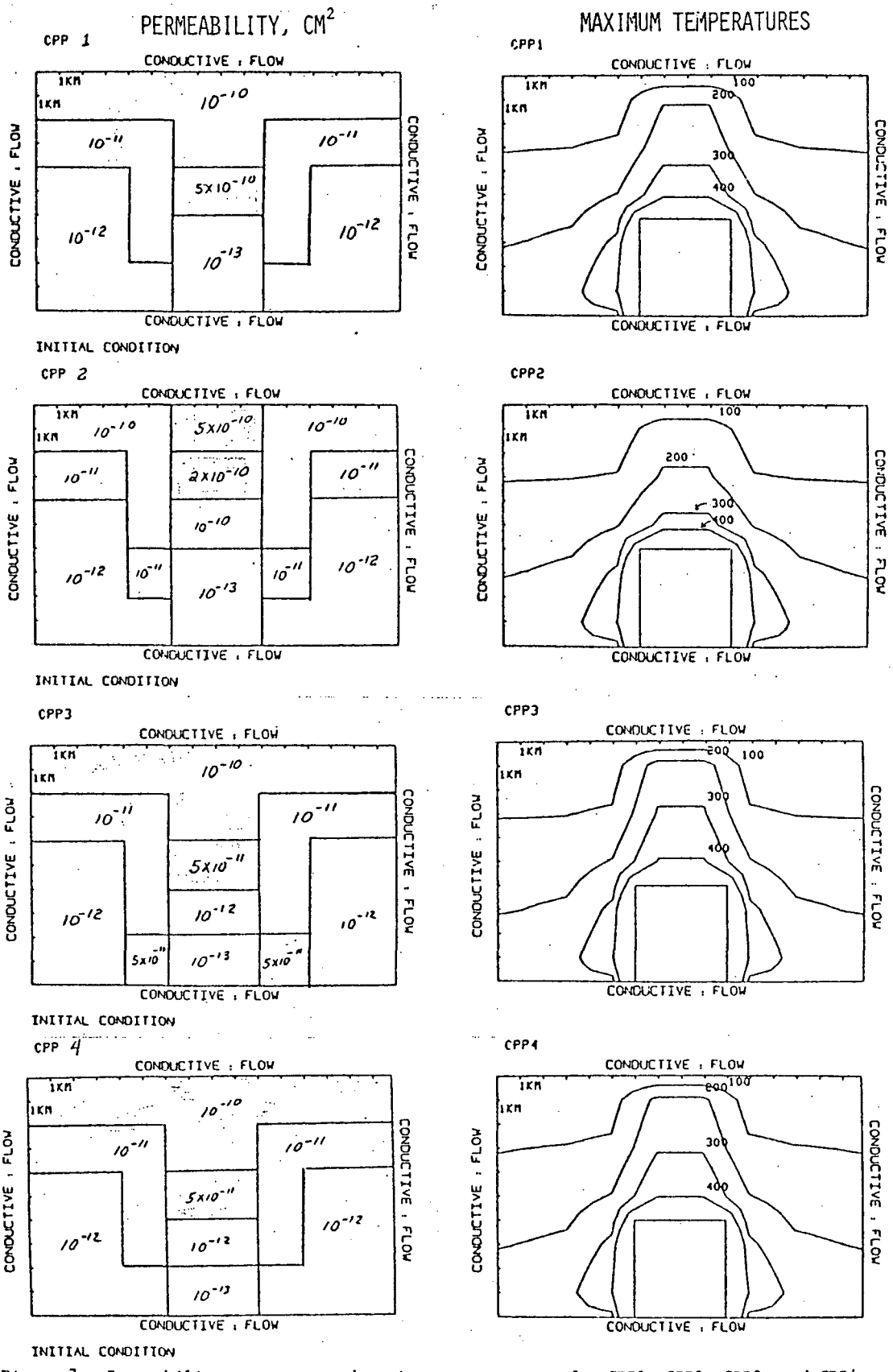

Figure 7. Permeability structure and maximum temperatures for CPP1, CPP2, CPP3, and CPP4. Permeability is in cm^{-2} and temperatures in °C.

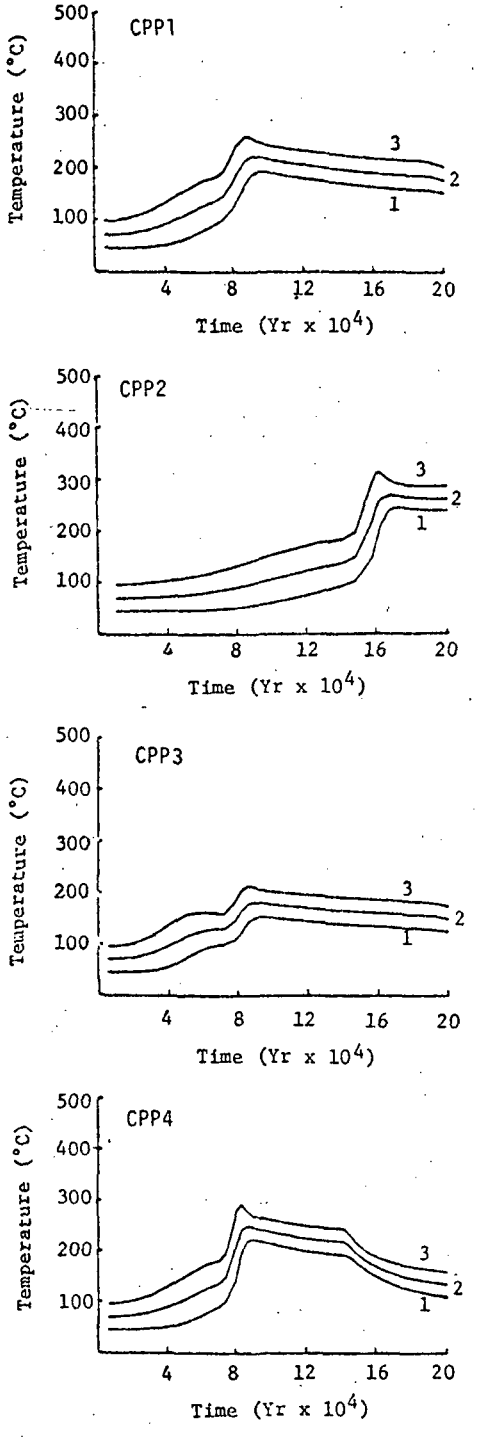

Figure 8. Temperature-time plots at 1, 2, and 3 km below surface directly above the heat source for models CPP1, CPP2, CPP3, CPP4.

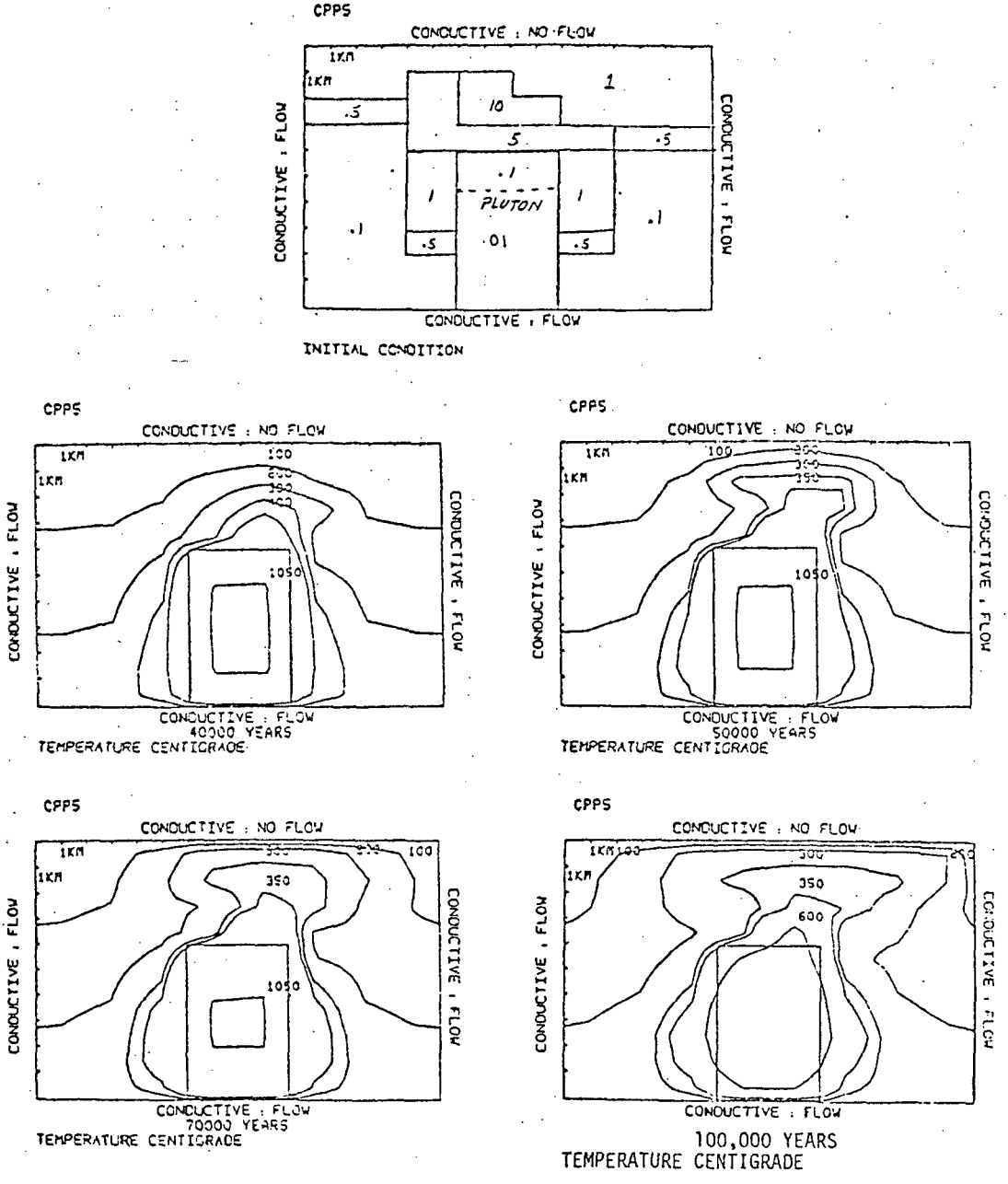

Figure 9. Initial condition and temperatures for four time steps. Model CPP5. Permeability in md.

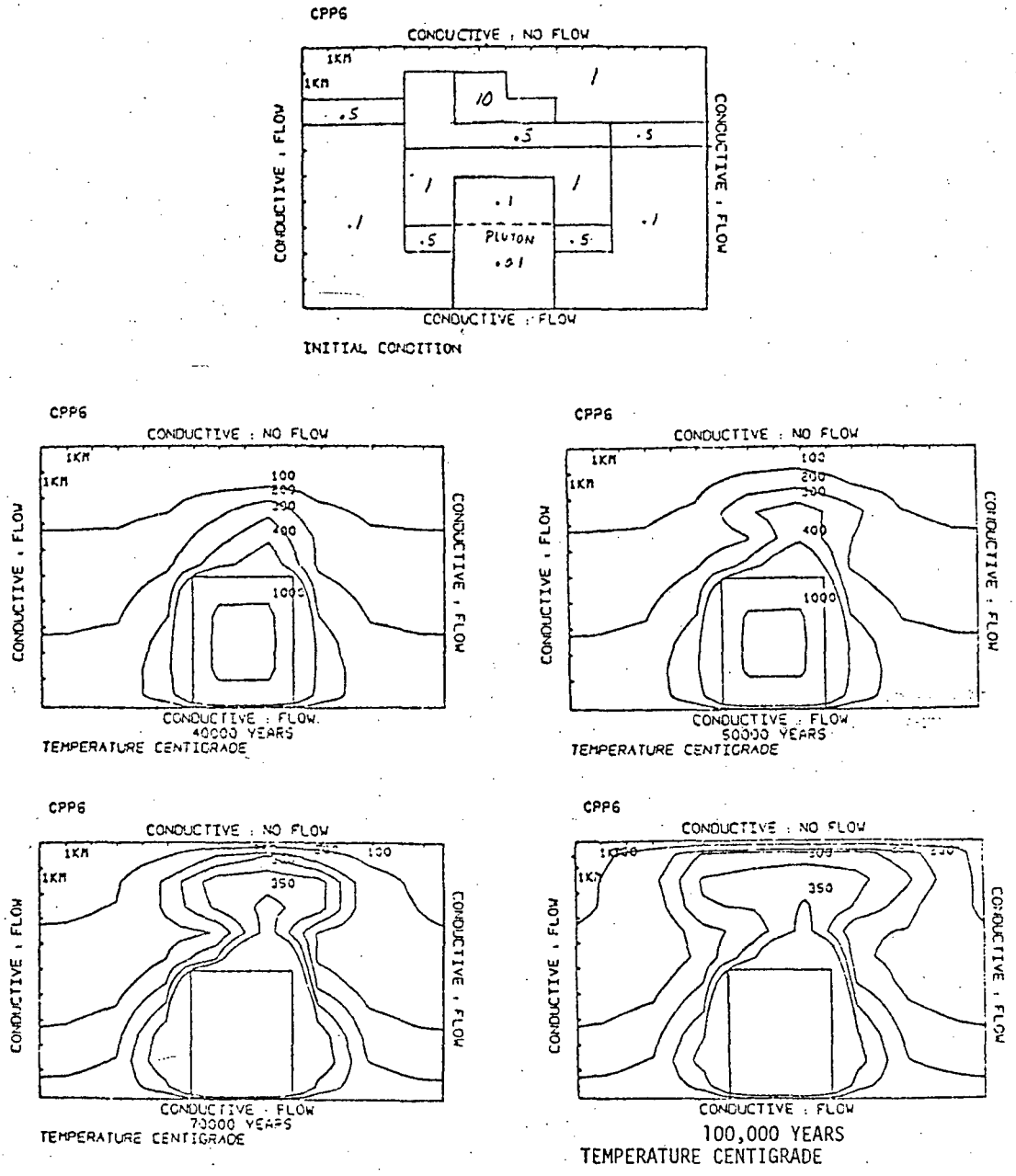

Figure 10. Initial condition and temperatures for four time steps. Model CPP6. Permeability in md.

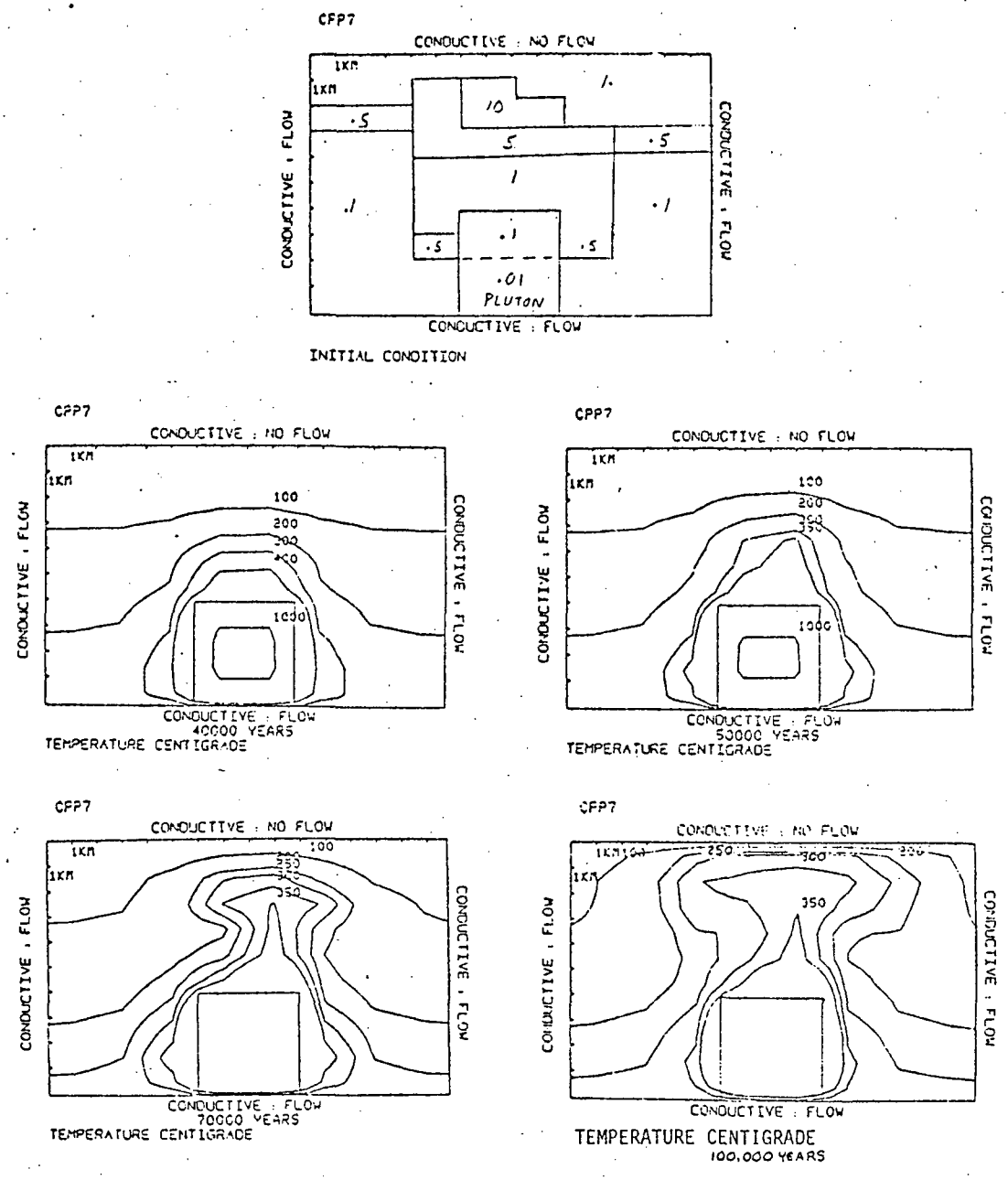

Figure 11. Initial condition and temperatures for four time steps. Model CPP7. Permeability in md.

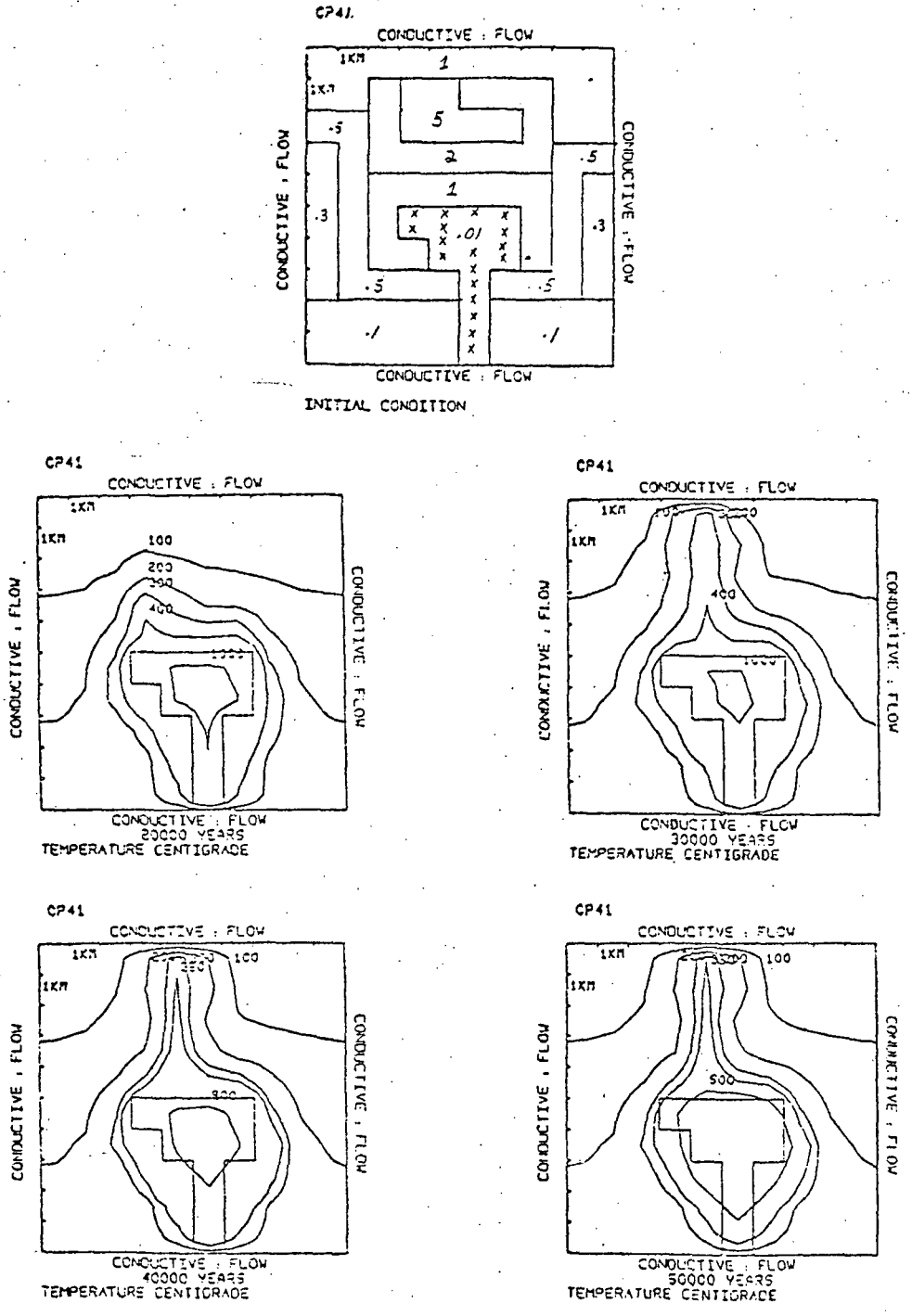

Figure 12. Initial condition and temperatures for four time steps. Model CP41. Permeability in md.

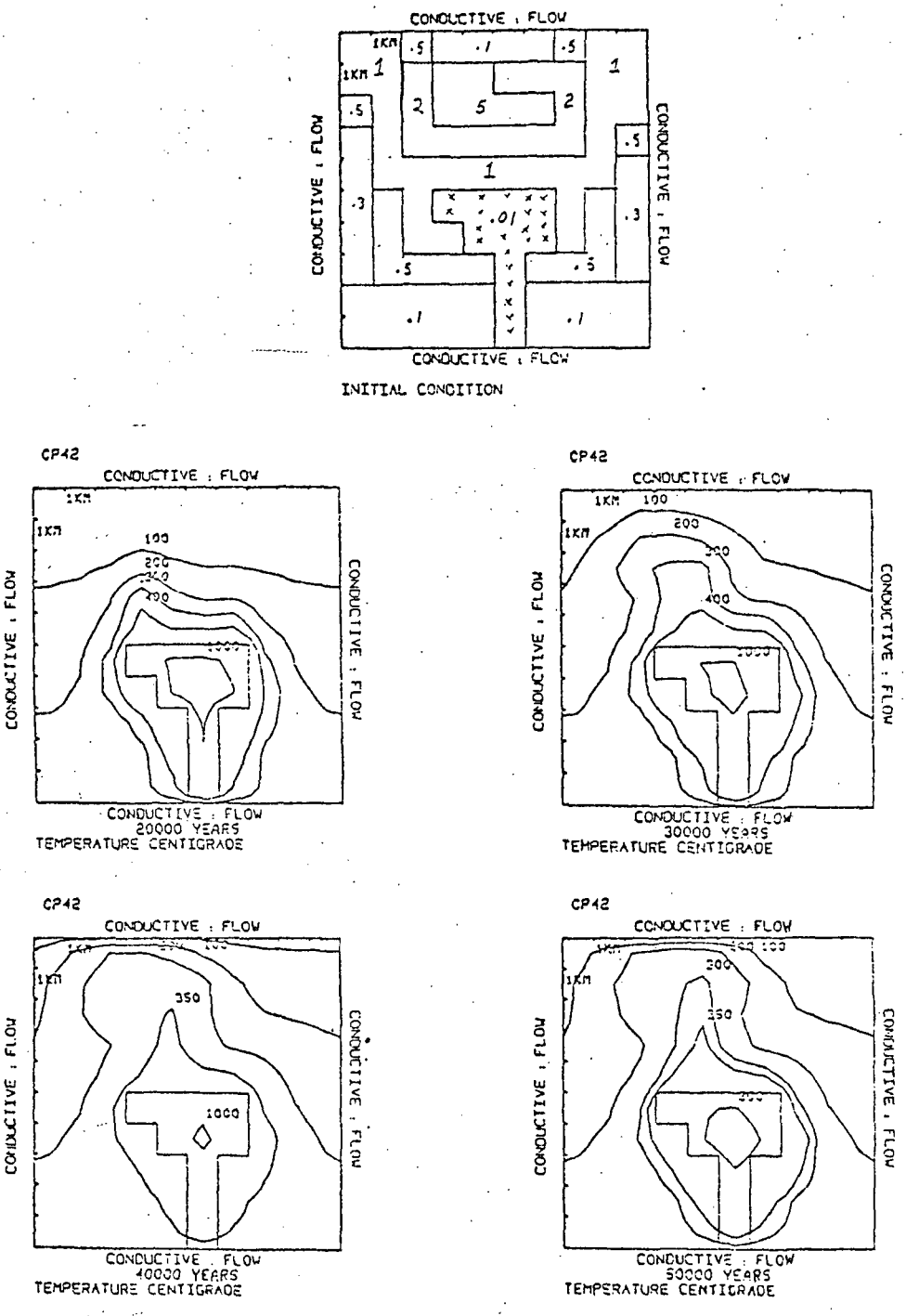

Figure 13. Initial condition and temperatures for four time steps. Model CP42. Permeability in md.

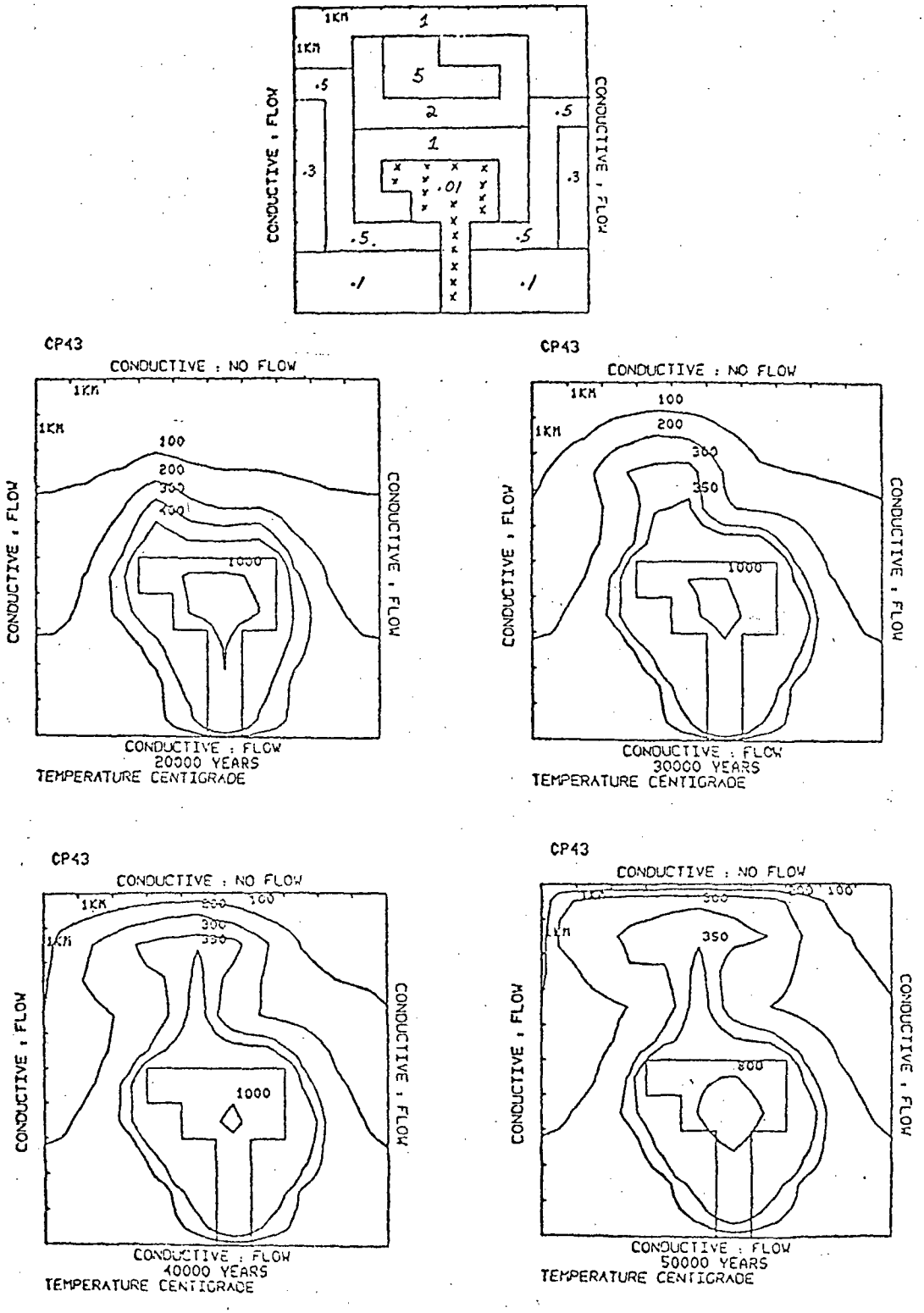

Figure 14. Initial condition and temperatures for four time steps. Model CP43. Permeability in md.